

Research on the vibration noise matching strategy of range-extended electric vehicle

Hongjun Zhang¹, Xiangnan Shi², Jingchang Chen³

^{1,2}YibinCowin Automobile Co., Ltd., Changjiang North Road, No. 7, Yibin, China

³China Automotive Engineering Research Institute Co., Jinyu Street, No. 9, Chongqing, China

¹Corresponding author

E-mail: ¹zhanghongjunllc@126.com, ²shixiangnan@newcowin.com, ³chenjingchang@caeri.com.cn

Received 28 August 2024; accepted 20 October 2024; published online 12 December 2024

DOI <https://doi.org/10.21595/vp.2024.24497>



71st International Conference on Vibroengineering in Riga, Latvia, December 12-13, 2024

Copyright © 2024 Hongjun Zhang, et al. This is an open access article distributed under the Creative Commons Attribution License, which permits unrestricted use, distribution, and reproduction in any medium, provided the original work is properly cited.

Abstract. Range-extended electric vehicles (REEVs) face more intricate noise, vibration, and harshness (NVH) challenges compared to traditional fuel and pure electric vehicles, primarily due to the complexities introduced by range extender control strategies. Poorly designed control logic can result in issues such as excessive noise during acceleration and engine roar, which are not only costly to rectify but also time-consuming. This article simplifies the theoretical model of range extender systems by treating the range extender as a single excitation source. By monitoring the vehicle's overall status, the system adjusts the output torque and crankshaft speed to evaluate the vibration and noise at critical points within the vehicle. This proactive approach helps to preemptively optimize NVH performance under various operating conditions, thereby minimizing the need for subsequent adjustments to the suspension, transmission, intake, and exhaust systems. As a result, it significantly reduces costs and accelerates the project's development timeline.

Keywords: range-extended electric vehicle, fuel economy, vibration noise, matching strategy.

1. Introduction

In the face of global climate and energy crises, electric vehicles (EVs) have attracted significant attention from major automakers for their substantial benefits in energy conservation and environmental sustainability. However, the limitations of power batteries, including low energy density, lengthy charging times, and limited range, have hindered the adoption of EVs [1]. Range-extended electric vehicles (REEVs) offer an innovative technological solution, reducing the range anxiety of pure EVs with the inclusion of a range extender system. This feature significantly enhances the driving range and simultaneously reduces engine fuel consumption.

Control strategies for range extender systems are predominantly centered on optimizing fuel economy. For instance, Liu and Tian [2] focused on enhancing the economic performance of REEVs through the selection of range-extender engines, specifically validating the efficacy of Miller cycle homogeneous charge compression ignition (HCCI) engines. Zhang and Li [3] employed a dynamic programming algorithm to explore the global optimal control strategy under various operating conditions, with fuel economy as the primary objective.

Nevertheless, customer acceptance of REEVs is largely contingent upon their noise, vibration, and harshness (NVH) characteristics, which must be competitive with those of traditional fuel and pure electric vehicles [4-5]. The introduction of range extenders introduces more complex NVH issues, such as increased acceleration noise and engine roar. Once the control strategy calibration is set, modifications are challenging and often require passive adjustments to the suspension, transmission, intake, and exhaust systems, which are costly and time-consuming.

Researchers like Wu [6] have examined the impact of turbochargers' high compression ratios and rapid combustion speeds on NVH performance, while Long [7] proposed solutions to reduce noise associated with air-cooled turbochargers. Chen et al. [8] introduced an adaptive fuzzy energy management strategy using an Improved Genetic Algorithm-Back Propagation (IGA-BP) neural network, which showed promising results in fuel economy and comfort. Hu and Zhang [9]

evaluated different engine control strategies through simulations, proposing strategies that align with user expectations regarding fuel consumption, emissions, and NVH.

Wang [10] conducted a comprehensive bench test to validate the vibration and noise characteristics of turbochargers, optimizing their control strategy through a multi-objective optimization approach. International research, such as that by Millo et al. [11] at Politecnico di Torino, has also delved into optimizing the vibration and noise of REEVs through energy management strategy refinement. Rodrigues et al. [12] have redesigned the energy management control strategy of the range extender to lessen the NVH impact on driving experience.

Despite these efforts, the performance variability of vehicle vibrations under different range extender control strategies has received limited systematic experimental validation in the literature. This study aims to bridge this gap by simplifying theoretical model derivations and analyzing extensive experimental data across various vehicle conditions. The goal is to establish a method for optimizing range extender system control strategies early in the vehicle development process. By identifying NVH (noise, vibration, and harshness) avoidance points, the study formulates a final control strategy that balances fuel economy with overall vehicle NVH performance. Furthermore, optimizing and iterating the range extender's calibration and matching strategy during the early stages of project development can significantly reduce subsequent adjustments to the suspension, transmission, intake, and exhaust systems, thereby cutting costs and accelerating the development timeline.

2. Problem description

The range extender system serves as both a source of vibration and noise. In this study, which primarily examines the influence of range extender system control strategies on NVH, the system is simplified to a single excitation source. The overall vehicle response to vibration and noise excitation is characterized by the vibration at the steering wheel at the driver's noon position and the seat rail, while noise is measured adjacent to the driver's right ear and the left ear of the rear right seat occupant.

For the exciter system, the excitation level represented externally varies with the change in effective power output of the exciter per unit time. The expression for the exciter effective power P_e is as follows:

$$P_e = \frac{T_e n}{9550} \text{ kW}, \quad (1)$$

where T_e denotes the effective torque, Nm; n denotes the crankshaft speed, r/min.

Therefore, the impact of the range extender system control strategy on the vibration and noise at key points in the vehicle can be further simplified to the matching control between the range extender system's effective output torque T_e and the crankshaft speed n . Chen et al. [13] have studied the impact of different ramp rates of crankshaft speed on the range extender, showing that there are significant differences in key point noise and vibration in the vehicle under different ramp rates.

3. Test validation

This study investigates the matching strategy of the range extender system by adopting fixed effective torque T_{ei} to change the crankshaft speed n at a fixed rate, thereby changing the excitation force of the range extender system. The method of obtaining the vibration noise of key response points inside the vehicle under effective torque excitation is detailed in Eq. (2):

$$\begin{pmatrix} T_{em}n_1 & T_{em}n_2 & \cdots & T_{em}n_{m-1} & T_{em}n_m \\ \vdots & \ddots & & \ddots & \vdots \\ T_{e1}n_1 & T_{e1}n_2 & \cdots & T_{e1}n_{m-1} & T_{e1}n_m \end{pmatrix}. \quad (2)$$

Under a fixed effective torque T_{e1} , the range extender's crankshaft speed n is increased from n_1 to n_m over a fixed time t , leading to the identification of the vibration and noise generated by the range extender system's effective torque T_{e1} within the vehicle cabin. Similarly, with the fixed effective torque T_{e2} , the range extender's crankshaft speed n is increased from n_1 to n_m over the same fixed time t , leading to the identification of the vibration and noise generated by the range extender system's effective torque T_{e2} within the vehicle cabin.

In this study, the prototype range extender system is selected based on the vehicle model, with T_{ei} set to 10 Nm and 160 Nm respectively, taking one measurement point every 5 Nm increment of T_{ei} ; n is set to 900 rpm and 4000 rpm respectively; the acceleration time t for speed is fixed at 30 seconds to simulate the driving habit of users with small throttle usage.

Test instrument requirements: test software using LMS Testlab test system; The three-way acceleration vibration sensors should be calibrated within the calibration validity period, and the microphones should be calibrated as necessary before the test; Set a reasonable sampling frequency and analysis bandwidth to ensure that there are enough spectral lines in the analysis bandwidth.

4. Analysis of test results

The working conditions of the range extender system for electric vehicles can be divided into idle charging conditions and driving charging conditions based on whether the vehicle is stationary or moving. To analyze the influence of the range extender system's control strategy on NVH (noise, vibration, and harshness), test data analysis is conducted separately for both idle charging conditions and driving charging conditions.

4.1. Idle charging condition test results analysis

Based on the effective power range required for idle charging conditions of the range extender system, idle charging condition data analysis is carried out for the ranges of $n = [900, 1500]$ r/min and $T_e = [10, 70]$ Nm.

a) Idle charging vibration data analysis.

As depicted in Fig. 1, the vibration of the range extender body escalates with increasing speed, particularly within the range of $n = [900, 1500]$ r/min. Additionally, within the torque range of $T_e = [10, 70]$ Nm, the body's vibration intensifies, with a more rapid increase observed at lower speeds compared to higher speeds.

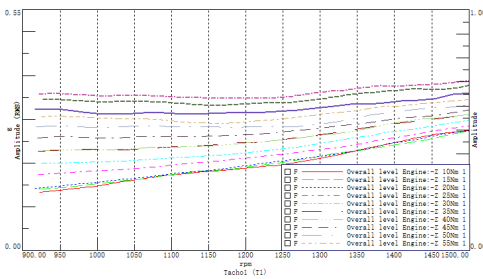


Fig. 1. Engine body vibration

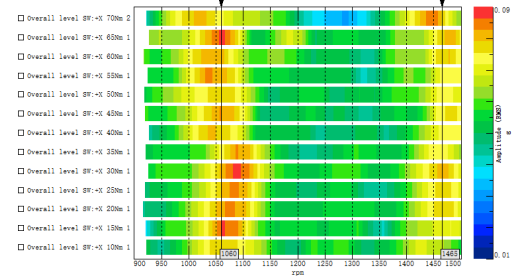


Fig. 2. X-axis vibration at the noon position on the steering wheel

Fig. 2 illustrates that the X-directional vibration at the steering wheel's noon position remains

relatively consistent across the torque range of $T_e = [10, 70]$ Nm range. However, within the speed range of $n = [900, 1500]$ r/min, there are obviously peaks in the X-directional vibration at the noon position of the steering wheel at around (1060 ± 50) r/min and (1465 ± 25) r/min.

As shown in Fig. 3, the seat rail Z-axis vibration remains relatively stable in the range of $T_e = [10, 35]$ Nm. Vibration peaks exist at 1050 r/min and 1400 r/min, but the overall vibration peak is not significant. As the load increases in the range of $T_e = [40, 70]$ Nm, the vibration peaks at (1050 ± 50) r/min and (1400 ± 40) r/min significantly increase, with the vibration peak at (1050 ± 50) r/min being considerably larger than the one at (1400 ± 40) r/min.

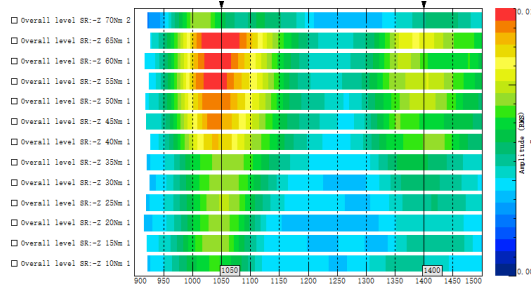


Fig. 3. Z-axis vibration of the seat rail

b) Idle charging noise data analysis.

Fig. 4 shows that the driver's right ear near noise levels are relatively high in the range of $n = [900, 1500]$ r/min, at various torques around (1200 ± 20) r/min; and in the range of $T_e = [10, 70]$ Nm, at torque segments of 30, 35 and 65 Nm, the noise levels are slightly higher at various speeds.

As shown in Fig. 5, the right ear of the rear right seat passenger is noisy between $n = [900, 1500]$ r/min, with torque > 50 Nm, around (1150 ± 30) r/min, and the sound pressure level is on the high side. In the range of $T_e = [10, 70]$ Nm, at 25 Nm at various speeds, the sound pressure level is obviously high.

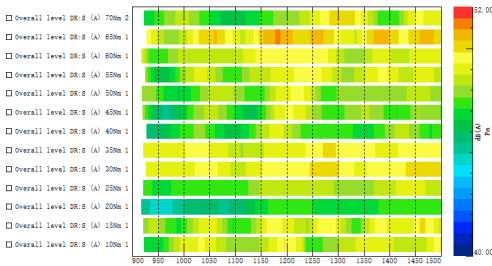


Fig. 4. Driver's right ear near noise

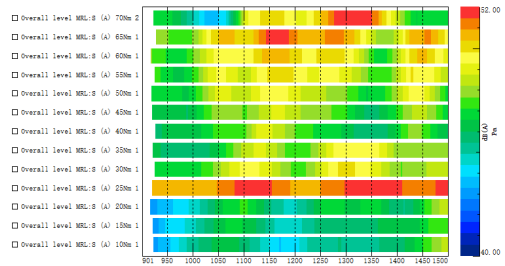


Fig. 5. The rear right seat passenger's left ear noise

4.2. Driving charging condition test results analysis

According to the overall control strategy of the range extender system fuel economy and the effective power range required for driving and charging conditions, the range of $n = [1500, 4000]$ r/min and $T_e = [10, 160]$ Nm is selected for data analysis of driving and charging conditions.

a) Driving charging vibration data analysis.

The main body of the range extender vibrates. In the range of $n = [1500, 4000]$ r/min, the overall vibration increases with the increase of the speed n . In the range of $[1800, 2000]$ r/min, there is a slight vibration mutation, mainly related to the intervention of the supercharger. In the range of $T_e = [10, 160]$ Nm, the overall vibration of the main body of the range extender increases

with the increase.

Fig. 6 depicts the vibrations at the steering wheel's noon position, showing obvious resonance bands that exist around (2340 ± 100) r/min and (3170 ± 100) r/min.

Fig. 7 indicates that within the range of $n = [1500, 4000]$ r/min, there is no obvious resonance band for the seat rail vibration. Regarding the Z-axis vibration of the seat rail, which is easily perceived by users, the overall vibration peak value is below 0.02 g when below the dividing line at 2400 r/min and 160 Nm and 3200 r/min and 10 Nm; while it is relatively higher above the dividing line at 2800 r/min and 160 Nm and 3600 r/min and 10 Nm.

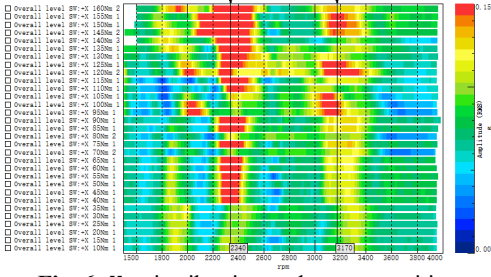


Fig. 6. X-axis vibration at the noon position on the steering wheel

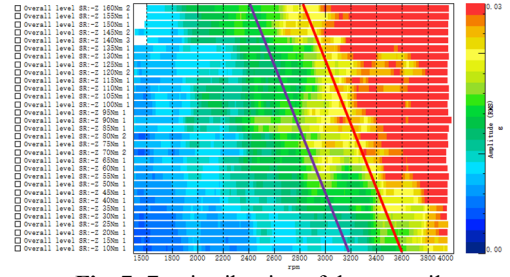


Fig. 7. Z-axis vibration of the seat rail

b) Driving charging noise data analysis.

Fig. 8 illustrates that the near-field noise of the range extender under driving and charging conditions generally increases with the increase of the speed n in the $T_e = [10, 120]$ Nm range. In the $T_e = [120, 160]$ Nm range, within the $n = [1500, 2400]$ r/min range, the near-field noise of the range extender notably increases; within the $n = [2400, 4000]$ r/min range, the near-field noise of the range extender remains relatively stable with no significant changes.

Fig. 9 shows that under driving charging conditions, the noise next to the driver's right ear is mostly below 58 dB(A) when below the dividing line at 2200 r/min and 160 Nm, and 3000 r/min and 10 Nm; while for the dividing line above 2800 r/min and 160 Nm, and 3600 r/min and 10 Nm, most of the noise levels exceed 60 dB(A).

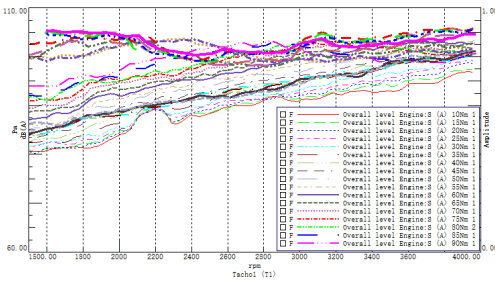


Fig. 8. Near-field noise of the range extender

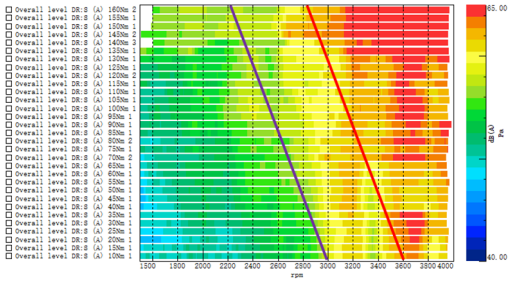


Fig. 9. Driver's right ear near noise

5. NVH strategy points of the range extender

Based on the above data analysis, the operational conditions avoidance points of NVH idle charging strategy and driving charging strategy for the range-extender electric vehicle can be summarized, as shown in Table 1 and Table 2.

6. Conclusions

This article simplifies the theoretical model, uses the range extender as a whole noise and vibration excitation source, applies a fixed effective torque, changes the crankshaft speed at a

fixed rate, thereby changing the excitation force of the range extender system, and covers the working conditions of the range extender system comprehensively. Under various operating conditions of the range extender, the vibration and noise performance of the key response points in the vehicle are obtained through experimental methods. In the early stage of the project's fuel economy calibration strategy, by inputting NVH performance strategy evasion points, it can inevitably take into account fuel economy while avoiding vibration and noise problems brought by the range extender earlier and more timely, thereby shortening the joint debugging period of the project. The matching strategy method studied in this article can guide the development of NVH performance matching of similar range extender electric vehicles.

Table 1. Idling Charging conditions range extender to avoid speed torque points

Key Points		Avoid speed and torque points
Vibration	Steering wheel	(1060±50) r/min and $T_e = [10, 70]$ Nm, (1465±25) r/min and $T_e = [10, 70]$ Nm
	Seat rail	(1050±50) r/min and $T_e = [40, 70]$ Nm, (1400±40) r/min and $T_e = [40, 70]$ Nm
Noise	Driver's right ear	(1200±20) r/min and $T_e = [10, 70]$ Nm, 30 Nm and $n = [900, 1500]$ r/min, 35 Nm and $n = [900, 1500]$ r/min, 65 Nm and $n = [900, 1500]$ r/min
	Rear right seat passenger's left ear	(1150±30) r/min and $T_e > 50$ Nm, 25 Nm and $n = [900, 1500]$ r/min, 65 Nm and $n = (1160±25)$ r/min, 70 Nm and $n = (1310±40)$ r/min

Table 2. Driving charging conditions range extender to avoid speed and torque points

Key points		Avoid speed and torque points
Vibration	Steering wheel	(2340±100) r/min and $T_e = [10, 160]$ Nm, (3170±100) r/min and $T_e > 90$ Nm
	Seat rail	n and $T_e > [2800$ r/min and 160 Nm, 3600 r/min and 10 Nm]
Noise	Driver's right ear	n and $T_e > [2800$ r/min and 160 Nm, 3600 r/min and 10 Nm]

Acknowledgements

The authors have not disclosed any funding.

Data availability

The datasets generated during and/or analyzed during the current study are available from the corresponding author on reasonable request.

Conflict of interest

The authors declare that they have no conflict of interest.

References

- [1] X. Y. Lin, H. B. Lin, L. Q. Zhai, and R. Xue, "PSO-fuzzy multi-objective control strategy based on PHEV charge-sustaining mode," *China Journal of Highway and Transport*, Vol. 29, No. 10, pp. 132–139, 2016, <https://doi.org/10.19721/j.cnki.1001-7372.2016.10.013>
- [2] Z. Liu and W. P. Tian, "Selection of engine as range extender in range-extended electric vehicle," *Automobile Technology*, Vol. 40, No. 3, pp. 21–24, 2018, <https://doi.org/10.19620/j.cnki.1000-3703.20170660>
- [3] B. Z. Zhang and K. F. Li, "Research on global optimal control strategy of PHEV based on dynamic programming," *Automobile Technology*, Vol. 40, No. 7, pp. 16–21, 2018, <https://doi.org/10.19620/j.cnki.1000-3703.20170789>
- [4] E. D. Tate, M. O. Harpster, and P. J. Savagian, "The Electrification of the automobile: from conventional hybrid, to plug-in hybrids, to extended-range electric vehicles," *SAE International*

Journal of Passenger Cars – Electronic and Electrical Systems, Vol. 1, No. 1, pp. 156–166, Apr. 2008, <https://doi.org/10.4271/2008-01-0458>

- [5] G. Friedrich and A. Girardin, “Integrated starter generator,” *IEEE Industry Applications Magazine*, Vol. 15, No. 4, pp. 26–34, Jul. 2009, <https://doi.org/10.1109/mra.2009.932592>
- [6] B. Wu, “NVH performance analysis of new energy vehicle range extender,” *Automobile Applied Technology*, Vol. 48, No. 7, pp. 26–29, 2023, <https://doi.org/10.16638/j.cnki.1671-7988.2023.07.005>
- [7] R. Long, “Research on sound insulation and heat dissipation performance of sound insulation cover for miniature electric vehicle range extender,” Chongqing University of Technology, 2023.
- [8] Y. Chen, C. Y. Wei, X. Y. Li, Y. L. Li, C. X. Liu, and X. Z. Lin, “Research on fuzzy energy management strategy for extended-range electric vehicles with driving condition identification,” *Automotive Engineering*, Vol. 44, No. 4, pp. 514–524, 2022, <https://doi.org/10.19562/j.chinasae.qcgc.2022.04.007>
- [9] P. Hu and H. Zhang, “Strategy of extended range electric vehicle based on user’s approval,” *Chinese Journal of Automotive Engineering*, Vol. 1, No. 6, pp. 455–463, 2011.
- [10] X. L. Wang, “The study on vibration and noise analysis and control of range-extender,” Shanghai University of Engineering Science, 2014.
- [11] F. Millo, L. Rolando, F. Mallamo, and R. Fuso, “Development of an optimal strategy for the energy management of a range-extended electric vehicle with additional noise, vibration and harshness constraints,” *Proceedings of the Institution of Mechanical Engineers, Part D: Journal of Automobile Engineering*, Vol. 227, No. 1, pp. 4–16, Oct. 2012, <https://doi.org/10.1177/0954407012457488>
- [12] M. Rodrigues, S. King, D. Scott, and D. Wang, “Advanced energy management strategies for range extended electric vehicle,” in *Symposium on International Automotive Technology*, Jan. 2015, <https://doi.org/10.4271/2015-26-0121>
- [13] J. Chen, X. Kong, and P. Li, “Analysis of the control strategy of range extender system on the vehicle NVH performance,” *Vibroengineering Procedia*, Vol. 33, pp. 90–95, Oct. 2020, <https://doi.org/10.21595/vp.2020.21681>